Liquid Crystals
Publication details, including instructions for authors and subscription information:
http://www.informaworld.com/smpp/title~content=t713926090

Smectogenic properties of *N,N'*-bis[(2-hydroxy-4-alkoxyphenyl)methylene]benzene-1,4-diamine liquid crystals with double lateral H-bonds

Guan-Yeow Yeap[a]; Tiang-Chuan Hng[a]; Wan Ahmad Kamil Mahmood[a]; Masato M. Ito[b]; Yamashita Youhei[b]; Yoichi Takanishi[c]; Hideo Takezoe[c]
[a] Liquid Crystal Research Laboratory, School of Chemical Sciences, Universiti Sains Malaysia, 11800 Minden, Penang, Malaysia [b] Department of Environmental Engineering for Symbiosis, Faculty of Engineering, Soka University, Hachioji, Tokyo 192-8577, Japan [c] Department of Organic and Polymeric Materials, Tokyo Institute of Technology S8-42, O-okayama, Meguro-ku, Tokyo 152-8552, Japan

To cite this Article Yeap, Guan-Yeow , Hng, Tiang-Chuan , Mahmood, Wan Ahmad Kamil , Ito, Masato M. , Youhei, Yamashita , Takanishi, Yoichi and Takezoe, Hideo(2006) 'Smectogenic properties of *N,N'*-bis[(2-hydroxy-4-alkoxyphenyl)methylene]benzene-1,4-diamine liquid crystals with double lateral H-bonds', Liquid Crystals, 33: 9, 979 — 986
To link to this Article: DOI: 10.1080/02678290600898419
URL: http://dx.doi.org/10.1080/02678290600898419

Liquid Crystals, Vol. 33, No. 9, September 2006, 979–986

Smectogenic properties of *N*,*N*′-bis[(2-hydroxy-4-alkoxyphenyl)methylene]benzene-1,4-diamine liquid crystals with double lateral H-bonds

GUAN-YEOW YEAP*†, TIANG-CHUAN HNG†, WAN AHMAD KAMIL MAHMOOD†, MASATO M ITO‡, YAMASHITA YOUHEI‡, YOICHI TAKANISHI§ and HIDEO TAKEZOE§

†Liquid Crystal Research Laboratory, School of Chemical Sciences, Universiti Sains Malaysia, 11800 Minden, Penang, Malaysia

‡Department of Environmental Engineering for Symbiosis, Faculty of Engineering, Soka University, Hachioji, Tokyo 192-8577, Japan

§Department of Organic and Polymeric Materials, Tokyo Institute of Technology S8-42, O-okayama, Meguro-ku, Tokyo 152-8552, Japan

(*Received 8 March 2006; accepted 22 May 2006*)

A series of eight liquid crystalline compounds, *N*,*N*′-bis[(2-hydroxy-4-alkoxyphenyl)methylene]benzene-1,4-diamines, has been synthesized and characterized. These homologous compounds differ in the length of terminal alkyl group C_nH_{2n+1} wherein *n* is an even number ranging from 4 to 18. The spectroscopic techniques, FTIR, ^{1}H NMR and ^{13}C NMR, were employed to characterize the molecular structure. The transition temperatures of all the title compounds and their mesophases were studied by differential scanning calorimetry and polarizing microscopy. All the compounds were smectogenic, exhibiting both tilted and non-tilted molecular orientation in their smectic phases. Further investigation to ascertain the anisotropic nature of subphases within the smectogenic region was carried out using X-ray diffraction.

1. Introduction

Molecules having symmetrical structures, in particular liquid crystal dimers, have received great attention as a class of mesomorphic materials because they differ from the conventional low molar mass mesogens in terms of repeating units in their molecular structures and properties [1]. By definition, these dimeric liquid crystals consist of two mesogenic groups connected via a flexible central spacer [2, 3]. They serve as models for semi-flexible main chain liquid crystal polymers due to their interesting physical properties such as the strong odd–even effects in the phase transition region [4]. Molecules in which the structure is composed of two flexible alkyl groups connected by a rigid mesogenic moiety i.e. the inverse of the dimer structure, are termed conventional low molar mass liquid crystals.

Chemical constitution has often been regarded as one of the major factors associated with mesomorphic behaviour [5]. In addition, hydrogen bonding plays a significant role in governing the thermal stability. It has generally been found that the presence of the hydroxyl group at the *ortho*-position leads to the formation of intramolecular hydrogen bonding, which in turn leads to an increase in the rigidity and thus in thermal stability of the mesophase [6, 7]. The influence associated with the presence of various lateral substituents attached to the mesogenic segment on the depression of the thermal stability of the mesophase has also been widely discussed [8–10]. The increased molecular breadth resulting from the attachment of lateral alkyl groups prevents the compounds from exhibiting higher-ordered phases, typically the smectic phases. The presence of the OH group, on the other hand, can enhance the stability of a molecule via intramolecular hydrogen bonding, and may also increase the lateral interaction between neighbouring molecules [11].

In order to investigate and explore further the unique properties of such compounds, we have synthesized a series of symmetrical liquid crystals with two azomethine groups in *para*-positions within the core which connect to aromatic rings at both ends, each with an *ortho*-hydroxyl group attached. These homologous

*Corresponding author. Email: gyyeap@usm.my or gyyeap_liqcryst_usm@yahoo.com

Liquid Crystals
ISSN 0267-8292 print/ISSN 1366-5855 online © 2006 Taylor & Francis
http://www.tandf.co.uk/journals
DOI: 10.1080/02678290600898419

members vary in terms of identical even-numbered alkyl groups at both terminal ends, ranging from C_4H_9 to $C_{18}H_{37}$. A previously reported homologue with $C_{10}H_{21}$ is included [12] in our discussion on the texture observation and transition temperature measurement.

2. Experimental

2.1. *Characterization*

FTIR analyses were performed on a Perkin-Elmer 2000-FTIR spectrophotometer. All samples were analysed in the form of KBr discs within the frequency range 4000–400 cm^{-1}. ^1H NMR and ^{13}C NMR analyses were carried out using Bruker 300 MHz and 400 MHz Ultrashield^{TM} FTNMR Spectrometers. The samples were prepared in $CDCl_3$ solution with the presence of TMS as internal standard. In order to facilitate the solubility of the title compounds in chloroform at room temperature, the temperature of the NMR samples was raised to 50°C using an internal heater. CHN micro-analyses were performed on a Perkin-Elmer 2400 LS series CHNS/O analyzer.

Textures were observed under a Carl Zeiss Axioskop 40 polarizing microscope equipped with a Linkam LTS350 hot stage in the Liquid Crystal Research Laboratory, School of Chemical Sciences, Universiti Sains Malaysia. The heating and cooling temperatures were monitored by a Linkam TMS94 temperature controller. Phase transition temperatures and enthalpies were determined with a Perkin-Elmer Pyris 1 DSC (Universiti Sains, Malaysia) and Shimadzu DSC-50 (Soka University, Japan) at heating and cooling rates of 5°C min^{-1}.

A representative sample was further analysed by X-ray diffraction (XRD), using a Rigaku RU-200 (CuK_α, 12 kW) and a temperature controller with an accuracy of ± 0.1°C. A sample cell consisted of a glass sandwich cell without rubbed polymer. The call gap was about 25 μm, and the thickness of the glass substrates was 150 μm. Temperature dependence of the layer thickness was measured by the conventional 2θ–θ method. 2D X-ray profiles were obtained using the imaging plate system R-AXIS. The camera length was calibrated by measuring stearic acid, and was determined to be 140 mm.

2.2. *Synthesis*

2,4-Dihydroxybenzaldehyde, *p*-phenylenediamine, 1-bromohexane, 1-bromododecane, 1-bromohexadecane and 1-bromooctadecane were purchased from Acros Organics, Belgium. 1-Bromobutane, 1-bromooctane, 1-bromodecane and 1-bromotetradecane were obtained from Merck, Germany. Potassium carbonate was purchased from Fisher Scientific, UK.

The syntheses of the intermediate compound **1** and the ultimate liquid crystal compounds **2**–**9** were carried out using the procedures summarized in scheme 1. The synthesis of each compound was identical, and representative only for compound characterization data are provided.

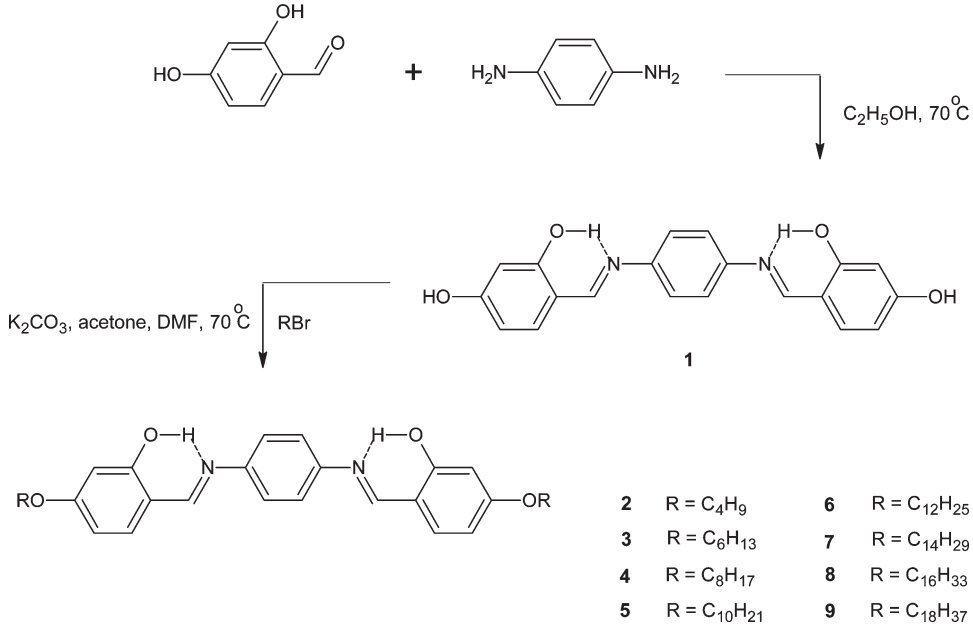

Scheme 1.

2.2.1. Synthesis of compound 1. A minimum ethanolic solution of *p*-phenylenediamine (1.081 g, 10.0 mmole) was added dropwise to a stirred 50 ml ethanolic solutionof 2,4-dihydroxybenzaldehyde (2.970 g, 21.5 mmol). The reaction mixture was then heated at 70°C whereupon a yellow precipitate was formed. This precipitate gradually turned to an orange colour on further heating. It was then heated under reflux for 1/2 h before the solvent was left to evaporate at room temperature. The solid substance thus isolated was then crystallized twice from ethanol to yield the desired intermediate compound; yield 79%. Elemental analysis: found, C 69.02, H 4.66, N 8.02; calculated ($C_{20}H_{16}N_2O_4$), C 68.96, H 4.63, N8.04%. IR (KBr), 3236 cm^{-1} (OH), 1621 cm^{-1} (C=N).

2.2.2. Synthesis of compound 2. The intermediate compound **1** (0.522 g, 1.5 mmol) was dissolved in a minimum of *N*,*N*′-dimethylformamide (DMF) containing K_2CO_3 (1.037 g, 7.5 mmol) and 40 ml acetone was added to this solution. The stirred solution was heated to 40°C; 1-bromobutane (0.452 g, 3.3 mmol) was then added dropwise and the mixture heated at 70°C for 16 h before evaporating off the acetone at room temperature. The resulting DMF solution was then poured into 50 ml water and the precipitate thus formed was filtered off and dried. It was washed with a cold mixture of DMF and acetone before being recrystallized from ethyl acetate to yield the final product; yield 72%. Elemental analysis: found, C 73.07, H 7.03, N 6.06; calculated ($C_{28}H_{32}N_2O_4$), C 73.02, H 7.00, N 6.08%. IR (KBr), 2955–2873 cm^{-1} (C–H alkyl), 1623 cm^{-1} (C=N), 1286 cm^{-1} (O–CH_2). ^{1}H NMR δ ($CDCl_3$), 0.99–1.04 ppm (t, 6H, CH_3), 1.47–1.86 ppm (m, 8H, CH_2), 4.02–4.06 ppm (t, 4H, O–CH_2), 6.49–6.50 ppm (d, 2H, Ar), 6.52 ppm (s, 2H, Ar), 7.26–7.29 ppm (m, 6H, Ar), 8.56 ppm (s, 2H, CH=N), 13.66 ppm (s, 2H, OH). ^{13}C NMR δ ($CDCl_3$), 14.23 ppm (CH_3), 19.60–31.51 ppm (CH_2), 68.35 ppm (O–CH_2), 101.95–133.89 ppm (Ar–C), 161.35 ppm (C=N), 164.07–164.29 ppm (Ar–C–O).

3. Results and discussion

3.1. *Thermal behaviour and texture observation*

The observed mesophases, transition temperatures and enthalpy values for compounds **2**–**9** are summarized in tables 1 and 2. All members are enantiotropic smecto-

Table 1. Transition temperatures (°C) and associated enthalpies (kJ mol^{-1}), in parentheses, of the *N*,*N*′-bis[(2-hydroxy-4-alkoxyphenyl)methylene]benzene-1,4-diamines during the heating cycle. (Cr=crystal; SmC=smectic C; SmA=smectic A; I=isotropic liquid).

Compound	Cr_1		Cr_2		Cr_3		SmC		SmA		I
2	•	160.7 (37.4)	•		—		—	302.6 (0.5)	•	325.9 (0.9)	•
3	•	133.5 (36.4)	•	170.9[a]	•	236.0[a]	•	275.2[a]	•	300.2 (1.7)	•
4	•	49.0 (12.3)	•	122.7 (37.9)	•	245.1[a]	•	269.8[a]	•	281.4 (6.6)	•
5	•	79.0 (20.9)	•	118.2 (42.4)	•	255.7[a]	•		—	264.9 (8.8)	•
6	•	95.0 (29.9)	•	115.2 (46.4)	•	219.6[a]	•		—	246.3 (7.6)	•
7	•	105.3 (38.7)	•	115.9,117.0[ba] (49.1)	•	235.2[a]	•		—	239.6 (9.9)	•
8	•	110.5 (28.2)	•	113.9,167.2[b] (39.7) (7.4)	•	212.6[a]	•		—	225.9 (8.3)	•
9	•	110.3 (3.0)	•	114.5,167.0[b] (103.5)(12.7)	•	204.3[a]	•		—	215.3 (1.5)	•

[a]Phase transition temperature obtained from optical microscopy (not detected by DSC due to the weak transition). [b]Additional crystal phase (Cr_4) which was observed using polarizing microscope

Table 2. Transition temperatures (°C) and associated enthalpies (kJ mol^{-1}), in parentheses, of the *N*,*N*′-bis[(2-hydroxy-4-alkoxyphenyl)methylene]benzene-1,4-diamines during the cooling cycle. (Cr=crystal; SmC=smectic C; SmA=smectic A; I=isotropic liquid).

Compound	Cr_1		Cr_2		Cr_3	SmC		SmA		I
2	•	121.0 (23.0)	•	133.0 (1.7)	—	•	208.0[a]	•	324.9[a]	•
3	•	100.5 (31.7)	—		—	•	250.3[a]	•	297.3 (1.8)	•
4	•	28.9 (3.0)	•	94.7 (35.9)	—	•	263.2[a]	•	279.6 (6.0)	•
5	•	64.4 (19.7)	•	92.2 (40.9)	—	•	263.4 (8.6)	—		•
6	•	82.9 (26.4)	•	95.1 (71.7)	—	•	243.8 (5.1)	—		•
7	•	94.4 (37.1)	•	103.3 (49.5)	—	•	237.6 (8.5)	—		•
8	•	102.5 (94.6)	—		—	•	222.8 (5.3)	—		•
9	•	112.0 (103.2)	—		—	•	215.3 (6.6)	—		•

[a]Phase transition temperatures obtained from optical microscopy (not detected by DSC due to the weak transition).

gens exhibiting the SmC phase during both heating and cooling except for compound **2**, which does not show the tilted phase on heating. On heating compound **2**, the Cr_2–SmA phase transition was detected at 302.6°C with an enthalpy of $0.5\,kJ\,mol^{-1}$, before isotropization occurred at 325.9°C. The enthalpy value for the Cr_2–SmA transition is much smaller than for Cr_1–Cr_2 ($\Delta H = 37.4\,kJ\,mol^{-1}$). This observation can be ascribed to the loss of some degree of positional order of molecules in the crystal lattice on the Cr_1–Cr_2 transition. With subsequent heating, the energy required to break the remaining positional order of the Cr_2, as well as its orientational order into the SmA phase, is very much lower. However, the temperature range of the SmA phase in compound **2** is found to be larger on cooling before transforming into a SmC phase at 208.0°C. Under polarized, the SmC broken fan-shaped texture is apparent prior to crystallization at 133.0°C. The other homologous compounds **3** and **4** similarly exhibit the focal-conic SmA phase (figure 1) in addition to the SmC phase. As the series ascends towards homologues with much longer alkyl chains at the terminal ends, the SmA phase is no longer observed but the characteristic of the SmC phase is preserved. A microscopic observation on the mesomorphic properties of compound **5** revealed that it actually exhibits the broken fan-shaped texture (figure 2) instead of the SmA phase reported by other researchers [12]. As the sample is heated, the crystalline subphase gradually turns into the SmC phase at 255.7°C before isotropization at 264.9°C.

Under polarized light, the enantiotropic compound **6** exhibits a unique filamentary texture which coalesces to form the broken focal-conic texture, indicating the presence of the SmC phase. This observation is in contrast to that reported for a salicylaldimine-based dimer with a C_4H_8 spacer, in which the phenomenon thus observed was regarded as the formation of SmA focal-conic domains [13]. This filament becomes longer as the temperature changes and, up to a certain length, buckling occurs to form the smectic phase (figure 3). It was then proposed that this filament was a SmA tube consisting of concentric cylindrical layers [14]. However,

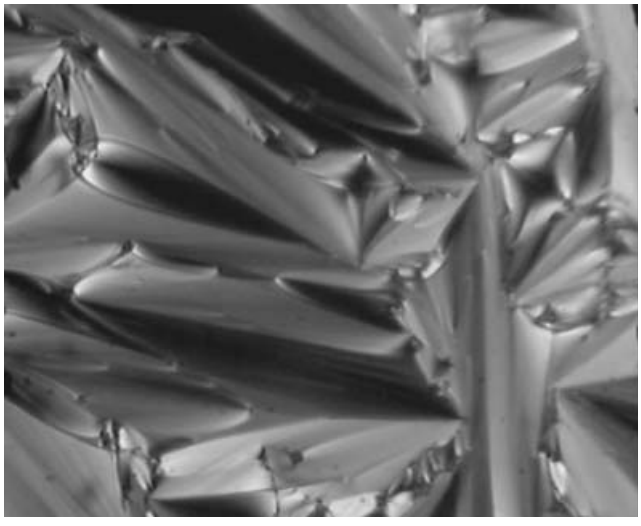

Figure 1. Photomicrograph showing the SmA focal-conic texture of compound **4** at 274.6°C during the second heating.

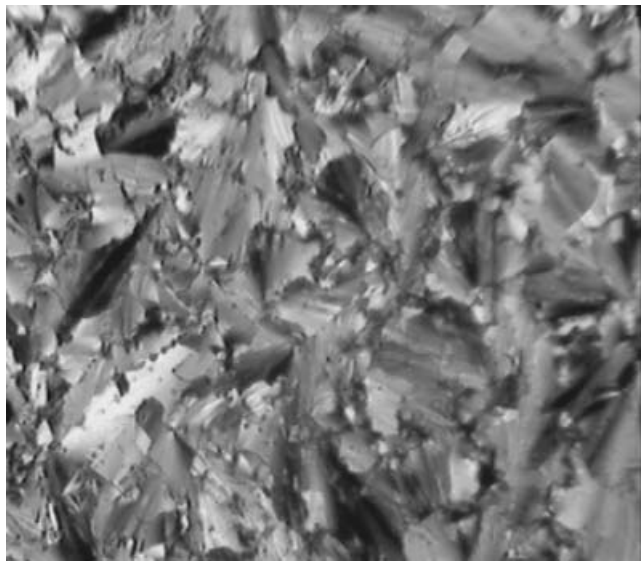

Figure 2. Photomicrograph of the SmC broken fan-shaped texture of compound **5** at 235.4°C during the second cooling.

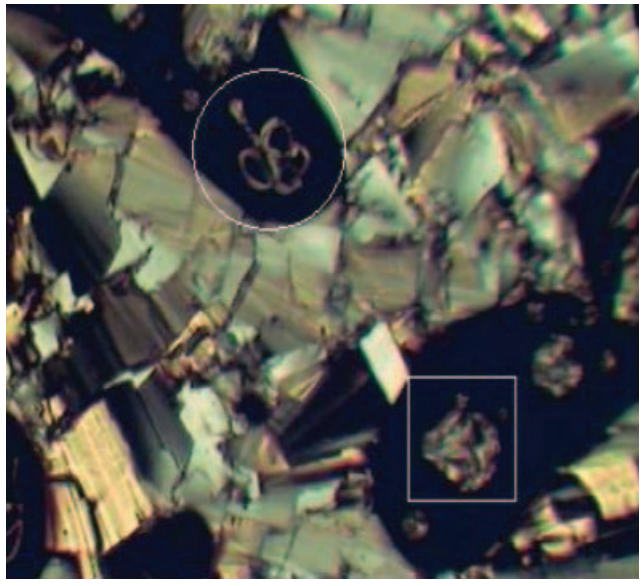

Figure 3. Photomicrograph showing the 'free-moving' filament (in circle) which coalesces to form the broken focal-conic texture (in square) of compound **6** at 174.4°C during the second heating.

the presence of the filaments we observed in the midst of the SmC phase suggests that the filamentary growth of the smectic tube is not exclusive for the SmA phase but could also be present in other smectic phases.

On further increasing the length of the terminal alkyl groups, the enantiotropic compounds **7**–**9** exhibit the SmC phase. From the isotropic phase with slow cooling at 3°C min^{-1}, a gradual appearance of batonnets within the matrix eventually led to the formation of the broken fan-shaped texture characteristic of the SmC phase. It is interesting to note that on further cooling of the same sample, repetitive examination on the hot stage revealed a slow disappearance of fine lines across the fans which originally constituted the SmC broken fan-shaped texture. This observation is rather unusual as the broken fan-shaped texture normally becomes even more apparent with decrease of temperature. This textural change was observed at a relatively low temperature of 134.1°C (compound **7**), 133.6°C (compound **8**) and 136.9°C (compound **9**). For compounds **8** and **9**, the enthalpy values of 8.6 and 13.1 kJ mol^{-1} were detected during the transition.

In our search for an explanation of this, an XRD study was carried out for representative compound **9**. XRD measurements show that only the SmC phase is present prior to crystallization during the cooling cycle, thus ruling out any possibility that a high order smectic phase is present. The two-dimensional XRD patterns for compound **9** are shown in figures 4 (*a*) and 4(*b*). From the profiles, at 126.0°C a sharp reflection is found in the low angle region whilst in the wide angle region, a diffuse peak is present [2, 15]. The layer spacing of 45.0 Å is determined from the first order reflection which corresponds to the molecular tilt angle of 37.5°, taking into account the molecular length of 56.7 Å (the calculated length of molecule with all-*trans* conformation is 58.7 Å) [16]. The result of XRD measurements for compound **9** is given in figure 5, in which the molecular layer spacing is plotted versus temperature. On cooling the isotropic phase, the SmC phase was observed at 215.3°C. At this temperature, the layer spacing is about 42.0 Å, which corresponds to a molecular tilt angle of 42.2° with respect to the layer normal. As the sample is cooled further, this angle decreased gradually to 36.3° before crystallization occurred at 112.0°C. The characteristic feature of increasing SmC layer spacing (decrease in tilt angle) with descending temperature has also been reported for cholesterol-containing liquid crystal dimers [1].

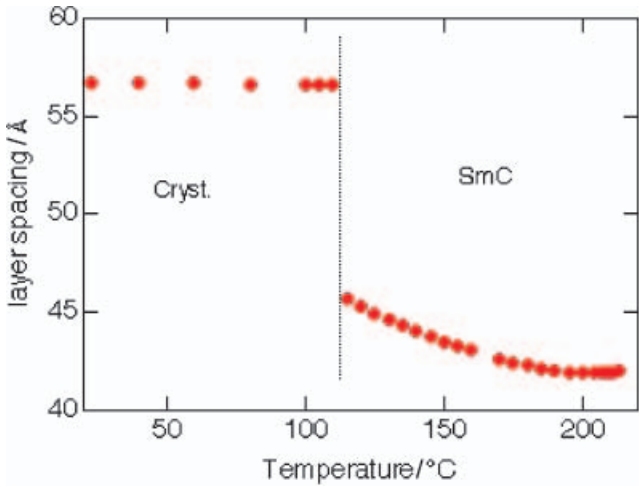

Figure 5. Dependence of molecular layer spacing on temperature for compound **9** in the crystal and SmC phases.

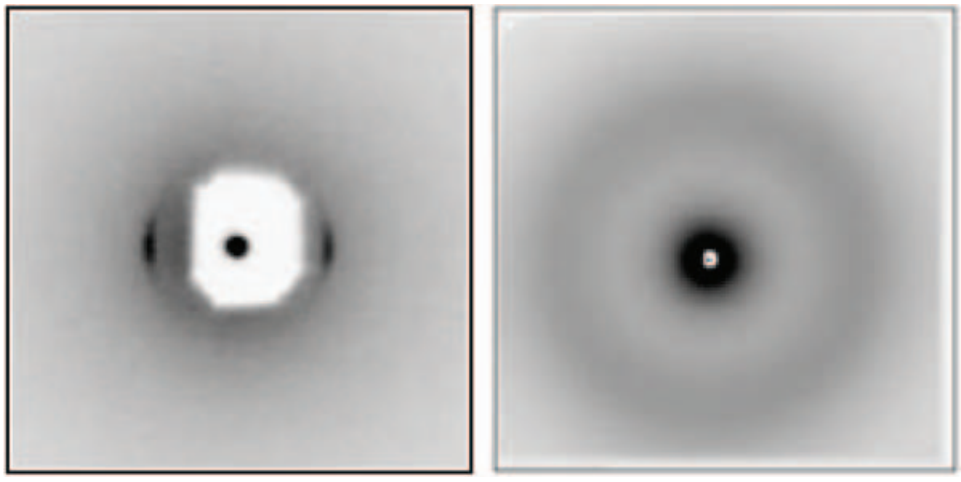

(*a*) (*b*)

Figure 4. X-ray diffraction patterns of compound **9** at (*a*) low angle and (*b*) wide angle, at 126.0°C.

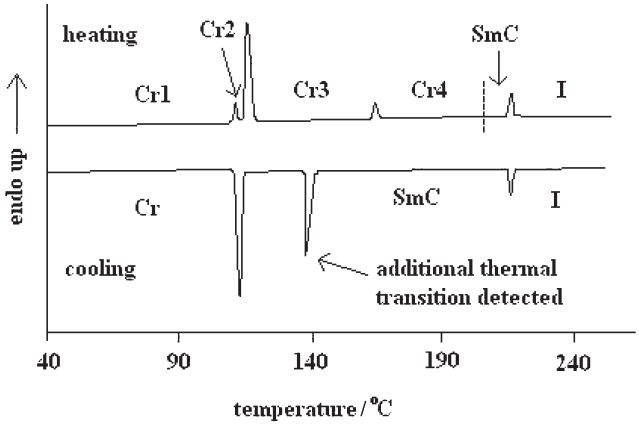

Figure 6. DSC trace of compound **9** showing various phase transitions.

The unusual phase transitions for compounds **7**–**9** were not included in tables 1 and 2, as the XRD experiment confirmed that only the SmC phase was present before crystallization. For compounds **7**–**9**, only the SmC phase is observed over a narrow range of temperature on heating. This could be ascribed to the fact that, unlike in the other lower members, crystal polymorphism becomes more apparent as the series is ascended, with the appearance of more than one crystal sub-phase with high thermal stability. During heating, the three highest members (**7**–**9**) exhibit another three different crystal phases most of which give rise to peaks in the DSC thermograms (figure 6). This observation is reminiscent of the findings of Yelamaggad *et al.*, who have reported a number of salicylaldimine-based symmetric dimers which also possess crystal polymorphism [15]. This unique behaviour may be caused by the limited mobility of the salicylaldimine moieties. One probable reason is that the presence of intramolecular hydrogen bonding stiffens the entire molecule; as a consequence, its fluidity is decreased. Even though these homologous members possess long alkyl groups at the terminal of the mesogenic core, the suppression of mesogenic properties, especially during cooling, is still very much pronounced. Thus, the overall mesophase range is greatly reduced from 191.9°C (compound **2**) to 107.7°C for the highest member (compound **9**).

Compounds **2**–**9** are different from the earlier reported analogues of 4-*n*-alkoxybenzaldehydes [17] because only the SmC phase is observed, regardless of the terminal flexible groups ranging from butyl to octadecyl. Although the previous study showed that there were higher ordered phases, other than the SmC reported for the benzaldehydes derivatives, the present investigation by XRD has confirmed that only the SmC phase appeared during cooling.

During heating, a trend in which the clearing points decrease as the number of terminal alkyl carbon atoms increases is observed. One probable reasons for this phenomenon is the reduction of molecular rigidity, which lowers the clearing point. Berdague *et al.* described this as a dilution of the core induced by the terminal chains [18]. As a result, the ability to fit into the smectic arrangement is also affected.

The observed smectogenic characteristics of the title compounds may be explained further by referring to the molecular structure of the dimers. The ^{1}H NMR analytical data of compound **3** shows the resonance of the *ortho* hydroxyl proton at $\delta = 13.56$–13.67 ppm. This observation is in agreement with the previously observed down-field shift of the hydroxyl proton resonance to $\delta = 13$–14 ppm, as the consequence of intramolecular hydrogen bonding [19, 20]. The intramolecular hydrogen bonds on both sides of the dimers resulted in a more rigid core which may adopt an almost coplanar orientation [21]. The planar orientation of the mesogenic core is especially likely to induce a smectic phase, as lateral interaction among molecules and the intermolecular force are enhanced in the smectic layers. For the homologues, it is also worthwhile to mention that the polarizability along the long axis of the molecule will be larger relative to that of laterally unsubstituted molecules [8].

The calculated polarizability values of compounds **2**–**9** (table 3) show an increase of 7.31×10^{-24} cm^3 with every addition of two methylene fragments at each terminal end when ascending the series. As the molecule becomes longer, the polarizability value is also higher because more atomic orbitals are available to construct the molecular orbitals. On the other hand, the presence of hydrogen bonds also contributes to the overall polarizability, as the electron density from the imine nitrogen atom is dispersed to the hydrogen atom of the OH group, which alters the charge distribution in the molecules. When these molecules arrange in adjacent layers, there will be stronger attraction in terms of London dispersion forces, whose intensity depend on the polarizability of the molecules. These forces play a

Table 3. Calculated polarizability values of compounds **2**–**9**.

Compound	Polarizability ($\pm 0.5 \times 10^{-24}$ cm^3)
2	53.18
3	60.49
4	67.80
5	75.11
6	82.42
7	89.73
8	97.04
9	104.35

significant role in maintaining the smectic layers, as molecules are held together with orientational order as well as positional order.

3.2. *Physical characterization*

From the FTIR spectra, it was observed that diagnostic bands of the alkyl groups were present in the frequency range 2849–2954 cm^{-1}. The relative intensity of these bands increased on ascending the series due to the increase of carbon number residing in the alkyl groups at both terminals. In the region 1621–1624 cm^{-1}, sharp bands contributed by the presence of azomethine (C=N) bonds were observed for all the compounds including the intermediate compound, **1**. This observation is in agreement with results obtained by Güner *et al.*, who had prepared a series of *N*-benzylideneanilines with azomethine group stretching frequency detected at 1619–1633 cm^{-1} [22]. The ether group of Ar–O–CH_2 at the two outer aromatic rings, however, gave rise to strong absorptions at1286–1289 cm^{-1}.

The FTIR spectroscopic study was further supported by the application of ^1H and ^{13}C NMR in an effort to elucidate the molecular structures. The following discussion on NMR chemical shifts is focused on compound **2** (with C_4H_9 terminal groups) as a representative for the series.

In the ^1H NMR spectrum of compound **2**, a triplet was observed at the high-field of δ=0.99–1.04 ppm, which can be assigned to the two sets of methyl protons of the terminal butyl groups. The two sets of methylene protons at respective terminals gave rise to a total of two multiplets within the range δ=1.47–1.86 ppm. At δ=4.02–4.06 ppm, another triplet was detected and was assigned to the methoxy protons adjacent to the methylene protons. The absorption of ten aromatic protons from four different distinguishable positions at the rings gave rise to a doublet, singlet and multiplet at δ=6.18–6.50, 6.52 and 7.26–7.29 ppm, respectively. The observed singlet is attributed to the presence of the lone aromatic proton located between two quaternary carbons at each side of the molecule. As such, no splitting was observed. At δ=8.56 ppm, a singlet assignable to the two azomethine protons was observed. Our results here are similar to those literature reports in which a singlet present in the range δ=8.45–8.57 ppm is attributed to the azomethine group [23]. Another singlet due to the absorption of the lateral hydroxyl protons was detected furthest down-field at δ=13.66 ppm.

The structural information of compound **2** was also inferred from ^{13}C NMR spectroscopy. The ambiguity of certain peak chemical shift assignments, especially at down-field, involving quaternary aromatic carbons was resolved via the COSY, HMQC and HMBC techniques. Whilst the signal attributed to the methyl carbon was observed at high-field at δ=14.23 ppm, the methylene carbons gave rise to another two peaks at δ=19.60–31.51 ppm. The methoxy carbons belonging to the flexible tails absorbed at δ=68.35 ppm. Subsequently, the various connecting aromatic carbons which consist of protonated and quaternary carbons (Ar–C–azomethine–C) were identified by the absorption in the range 101.95–133.89 ppm. The azomethine carbons gave rise to a strong absorption at 161.35 ppm. At further down-field, the two signals contributed by the aromatic (quaternary) carbons with direct connection to the oxygen atoms (Ar–C–O–CH_2 and Ar–C–OH) were detected at 164.07 and 164.29 ppm.

4. Conclusion

A series of eight smectogenic liquid crystal homologues *N*,*N*′-bis[(2-hydroxy-4-alkoxyphenyl)methylene]benzene-1,4-diamine, differing by the even-parity alkyl group terminals, were successfully isolated and characterized. All members exhibit high thermal stability owing to the existence of double intramolecular hydrogen bonding caused by the *ortho*-hydroxyl groups. The smectogenic characteristics of the homologues are significantly more apparent during the cooling transitions. For compounds **7**–**9**, a unique disappearance of fine lines on the SmC broken fans was observed under polarized light at relatively low temperature suggests the existence of a second mesophase; but the ambiguity was resolved using XRD. The XRD study confirms that SmC is the only mesophase present during cooling cycles for the three longest homologues. The smectogenic characteristics of the compounds were associated with intramolecular hydrogen bonds at the mesogenic core. The presence of the hydrogen bonds produces an almost coplanar orientation which is conducive for molecular packing within the smectic layers.

Acknowledgements

G.-Y. Y. thanks Universiti Sains Malaysia and the Malaysian Government, especially the Ministry of Science, Technology and Innovation (MOSTI), for the intensified research grant no. 305/PKIMIA/612923 and USM Short-Term grant no. 304/PKIMIA/636103. We are also grateful to all staff in the Research and Creativity Management Office (RCMO) in University Sains Malaysia for assistance and support given indirectly to make this project a success.

References

[1] R.W. Date, C.T. Imrie, G.R. Luckhurst, J.M. Seddon. *Liq. Cryst.*, **12**, 203 (1992).

[2] J. Jin, Y. Chung, J. Kang. *Mol. Cryst. liq. Cryst.*, **82**, 261 (1982).
[3] J.W. Emsley, G.R. Luckhurst, G.N. Shilstone, I. Sage. *Mol. Cryst. liq. Cryst. Lett.*, **102**, 223 (1984).
[4] A.T.M. Marcelis, A. Koudijs, Z. Karczmarzyk, E.J.R. Sudhölter. *Liq. Cryst.*, **30**, 1357 (2003).
[5] D. Vörlander. *Z. physik. Chem.*, **57**, 357 (1907).
[6] R.A. Vora, R. Gupta. *Mol. Cryst. liq. Cryst. Lett.*, **56**, pp. 31, R.A. Vora, R. Gupta (1979). In *Liquid Crystals*, S. Chandrasekhar (Ed.) p. 589, Heyden Verlag (1980).
[7] F. Perez, P. Berdague, P. Judeinstein, J.P. Bayle, H. Allouchi, D. Chasseau, M. Cotrait, E. Lafontaine. *Liq. Cryst.*, **19**, 245 (1995).
[8] A.K. Prajapati, R.A. Vora, H.M. Pandya. *Mol. Cryst. liq. Cryst.*, **369**, 37 (2001).
[9] S.L. Arora, J.L. Fergason, A. Saupe. *Mol. Cryst. liq. Cryst.*, **10**, 243 (1970).
[10] M.J.S. Dewar, J.P. Schroeder. *J. org. Chem.*, **30**, 2296 (1965).
[11] A. Hallsby, M. Nilsson, B. Otterholm. *Mol. Cryst. liq. Cryst.*, **82**, 61 (1982).
[12] P. Berdague, J. Courtieu, P.M. Maitlis. *Chem. Commun.*, 1313 (1994).
[13] C.V. Yelamaggad, Mathews Manoj, UmaS. Hiremath, GeethaG. Nair, D.S. Shankar Rao, S. Krishna Prasad. *Liq. Cryst.*, **30**, 899 (2003).
[14] H. Naito, M. Okuda, Zhong-Can . *Phy. Rev.ô E*, **55**, 1655 (1997).
[15] C.V. Yelamaggad, S. Anitha Nagamani, UmaS. Hiremath, D.S. Shankar Rao, S. Krishna Prasad. *Liq. Cryst.*, **29**, 1401 (2002).
[16] *ACD/Labs ChemSketch 8.00 Release*, Product version:8.17 (2005).
[17] J. Barberá, M. Marcos, J.L. Serrano. *Mol. Cryst. liq. Cryst.*, **149**, 225 (1987).
[18] P. Berdague, J.P. Bayle, M.-S. Ho, B.M. Fung. *Liq. Cryst.*, **14**, 667 (1993).
[19] B.I. Ostrovskii, A.Z. Rabinovich, A.S. Sonin, E.L. Sorkin, B.A. Strukov, S.A. Taraskin. *Ferroelectrics*, **24**, 309 (1980).
[20] E. Grech, J. Nowicka-Scheibe, Z. Olejnik, T. Lis, Z. Pawelka, Z. Malarski, L. Sobczyk. *J. chem. Soc., Perkin Trans.2*, **3**, 343 (1996).
[21] M. Marcos, E. Melendez, J.L. Serrano. *Mol. Cryst. liq. Cryst.*, **91**, 157 (1983).
[22] V. Güner, S. Bayari. *Spectrosc. Lett.*, **35**, 83 (2002).
[23] R. Achten, A. Koudijs, Z. Karczmarzyk, A.T.M. Marcelis, E.J.R. Sudhölter. *Liq. Cryst.*, **31**, 215 (2004).